Available online at www.sciencedirect.com

SciVerse ScienceDirect

Ceramics International 39 (2013) 6963–6969

CERAMICS INTERNATIONAL

www.elsevier.com/locate/ceramint

Nucleation, crystallization behavior and microstructure of mica glass-ceramics in the system $SrO \cdot 4MgO \cdot xAl_2O_3 \cdot 6SiO_2 \cdot 2MgF_2$ ($x=1$, 1.5 and 2)

Amit Mallik, Paritosh Kundu, Arunabha Basumajumdar*

Ceramic Engineering Division, Department. of Chemical Technology, University of Calcutta; 92, A.P.C. Road, Kolkata 700009, India

Received 16 January 2013; received in revised form 13 February 2013; accepted 13 February 2013
Available online 19 February 2013

Abstract

The effect of varying Al_2O_3 content on the crystallization and microstructure behavior of strontium containing glasses based on the system $SrO \cdot 4MgO \cdot Al_2O_3 \cdot 6SiO_2 \cdot 2MgF_2$ was investigated by differential thermal analysis (DTA), X-ray diffraction (XRD) and scanning electron microscopy (SEM). The glass transition temperature (T_g) and first crystallization peak temperature (T_p^1) reduced with decrease in the alumina content. Glasses with $x \geq 1.5$ exhibited a second crystallization peak temperature (T_p^2). The first crystallization peak temperature (T_p^1) corresponded to the formation of strontium fluorophlogopite and second crystallization peak temperature (T_p^2) corresponded to the formation of strontium aluminum silicate.

Keywords: B. Microstructure-final; D. Glass; D. Glass-ceramics

1. Introduction

The controlled crystallization of glass produced glass-ceramics. Glasses based on the system $K_2O \cdot MgO \cdot Al_2O_3 \cdot SiO_2 \cdot MgF_2$ typically crystallize to trisilicic alkaline phlogopite mica ($K \cdot Mg_3 \cdot Al \cdot Si_3 \cdot O_{10} \cdot F_2$) glass-ceramics. These glass-ceramics have an important feature, which made them machinable to a precise tolerance with traditional metal working tools [1].

These materials can be easily cut, drilled and turned with conventional tools. 'House of cards' structure of mica crystals leads to the desirable machinability because they cleave easily along the interfaces between layers while being machined [2–5].

Glass-ceramics based on alkaline earth fluorophlogopites, particularly barium fluorophlogopite, are claimed to have two to three times higher mechanical strength than those of the corresponding potassium fluorophlogopite glass-ceramics [6–8].

Greene et al. [9] investigated the $(1-Z)BaO{:}ZK_2O{:}(6-X)MgO{:}XMgF_2{:}(3-Q)Al_2O_3{:}QB_2O_3{:}8SiO_2$ system (where $Z=0$, 0.25, 0.5, 0.75, and 1.0, $X=2$, 2.5, and 3.0 and $Q=0$, 0.5, and 1.0) and observed that the substitution of barium by potassium results in increase in molar volume, co-efficient of thermal expansion and decrease in fractional glass compactness, microhardness and glass transition temperature values.

In an earlier work [10], present authors had studied the kinetics as well as crystallization behavior, microstructure and mechanical properties of the system $Ba_x \cdot K_{1-2x} \cdot Mg_3 \cdot Al \cdot Si_3 \cdot O_{10} \cdot F_2$ ($x=0.0$, 0.3 and 0.5), where it was observed that machinability and strength can be customized by judicious substitution of potassium by barium and also by the duration of heat treatment schedule

In another work [11], present authors had studied the kinetics as well as crystal growth with respect to fluorine content in the barium fluorophlogopite glass-ceramics based on the system $BaO \cdot 4MgO \cdot Al_2O_3 \cdot 6SiO_2 \cdot 2MgF_2$, where it was indicated that the crystallization of the glass was largely homogenous and fluorine promotes initial crystallization.

Mallik et al. [12] studied the effect of varying B_2O_3 content on the crystallization and microstructure behavior

*Corresponding author. Tel.: +91 9433459595; fax: +91 33 2351 9755.
E-mail address: a.basumajumdar@gmail.com (A. Basumajumdar).

0272-8842/$ - see front matter © 2013 Elsevier Ltd and Techna Group S.r.l. All rights reserved.
http://dx.doi.org/10.1016/j.ceramint.2013.02.033

of barium containing glasses based on the system $BaO \cdot 4MgO \cdot Al_2O_3 \cdot 6SiO_2 \cdot 2MgF_2$, where it was indicated that the increase in B_2O_3 content reduces both glass transition temperature (T_g) and crystallization temperature (T_p) as well as addition of B_2O_3 tends to promote grain growth of fluormica flakes by increasing the fluidity of the growth medium.

Beall [13] undertook the first study of the alkaline earth fluormica glass-ceramics. Later on Hoda and Beall [14] investigated glasses of different compositions containing any two of the following cations—barium, calcium and strontium, based on fluorophlogopite stoichiometry. Most of the compositions were susceptible to crystallization during casting.

Henry and Hill [15,16] have shown that reduction in alumina content in the system $8SiO_2 \cdot YAl_2O_3 \cdot 4MgO \cdot 2MgF_2 \cdot BaO$ ($1.5 \leq Y \leq 3$) reduces the glass transition temperature and first crystallization peak temperature, and promotes bulk crystal nucleation. The glasses with high alumina contents gave rise to feathery microstructures that did not coarsen readily to give blocky crystals of high aspect ratio and therefore could not produce the classic 'house of cards' microstructure. Hardness and machinability were found to be highly dependent on the formation of an interconnected 'house of cards' microstructure.

No reference has been noticed by the authors in respect of any work on the system of strontium containing mica glass-ceramics. The purpose of this study is to characterize the crystallization mechanism and microstructure with the variation of alumina content in the strontium based fluorophlogopite glass-ceramics system.

2. Experimental

2.1. Glass synthesis

The glass-forming compositions studied are represented by the following generic formula:

$$SrO \cdot 4MgO \cdot xAl_2O_3 \cdot 6SiO_2 \cdot 2MgF_2$$

where x varies among 1.0, 1.5 and 2.0 as shown in Table 1. For this study, the glasses were synthesized using the analytical grade reagents, strontium carbonate ($SrCO_3$), silica (SiO_2), magnesium carbonate ($MgCO_3$), alumina (Al_2O_3), magnesium fluoride (MgF_2) and boric acid (H_3BO_3) from E. Merck, **and they were** mixed thoroughly in an attrition mill. In all the batches, 2 wt% B_2O_3 as H_3BO_3, was added to reduce the viscosity and thereof to increase the rate of diffusion of different ionic species in glass, which may result in the natural tendency toward directional growth of crystals [9]. Glass batches were melted in a platinum crucible in an electrically heated furnace and the melt was kept at the maximum melting temperature of 1500 °C for 2 h with occasional stirring with a platinum rod to homogenize the melt. The melts were poured into a preheated iron mold to make glass blocks of about 60 mm × 25 mm × 10 mm dimension. After releasing from the mold, the glass blocks were immediately transferred to an annealing furnace operating at a temperature 50 °C below the midpoint of the glass transition region and held for 1 h at the temperature followed by natural cooling to room temperature.

Table 1
Chemical composition of glass (in wt%).

Batch	SrO	MgO	Al_2O_3	SiO_2	MgF_2	B_2O_3
SR1	12.22	19.02	12.00	42.53	14.23	2.00
SR2	11.54	17.94	16.98	40.12	13.42	2.00
SR3	10.92	16.98	21.44	37.97	12.69	2.00

The annealed block was cut into pieces to about 1–2 mm thicknesses with a precision low speed cutting machine (Buehler). These cut samples were fired at 710 °C for 2 h for nucleation. Samples after nucleation were heated to corresponding crystallization temperature at a rate of 2 °C/min and samples were kept at the crystallization temperatures for 5 h.

2.2. Characterization techniques

2.2.1. Differential thermal analysis (DTA)

Differential thermal analysis (DTA) was done using a Shimadzu DT40 thermal analyzer with α-alumina powder as a reference material. Four different glasses were ground to powder of ~75 μm suitable for DTA study. Non-isothermal experiments were performed by heating ~17 mg glass sample at a heating rate of 10 °C/min in the temperature range from ambient to 1000 °C.

2.2.2. X-ray diffraction (XRD)

Three heat treatment temperatures were chosen for each batch to investigate crystallization behavior by X-ray powder diffraction. All samples were heat treated at a heating rate of 10 °C/min to the nucleation temperature (as mentioned in Section 2.1), soaked for 2 h at this temperature, heated again at 2°/min to the corresponding crystallization temperature and kept at that temperature for 5 h followed by natural cooling to room temperature. Samples from all the above mentioned glasses were ground to ~75 μm. XRD experiments were performed by an X-ray diffractometer (PW 1830; PANalytical) using Ni filtered Cu $K\alpha_1$ radiation with scanning speed of 2° (2θ) per minute. Diffraction pattern was recorded within Bragg angle range $10^\circ < 2\theta < 70^\circ$ and phases were identified by JCPDS numbers (ICDD–PDF2 database).

2.2.3. Scanning electron microscopy (SEM)

Samples heat treated at all the five crystallization temperatures (heating schedule as mentioned earlier) were studied to investigate microstructural development with back scattered electron imaging (BEI) mode in a scanning electron microscope Hitachi, S3400N, Japan. Samples

were polished with diamond paste and were etched chemically by 5% HF solution for 15 s.

3. Result and discussion

3.1. Differential thermal analysis (DTA)

DTA curves for the three glass samples performed at a heating rate of 10 °C/min are shown in Fig. 1. The nucleation and crystallization temperature were determined from DTA analysis of glass samples. The glass transition temperature (T_g) and first crystallization peak temperature (T_p^1) reduced with decrease in the alumina content. Glasses with $x \geq 1.5$ exhibited a second crystallization peak temperature (T_p^2). First crystallization peak temperature (T_p^1) corresponded to the crystallization of strontium fluorophlogopite and second crystallization peak temperature (T_p^2) corresponded to the crystallization of strontium aluminum silicate. The amplitude of the second crystallization peak temperature (T_p^2) reduced and eventually disappeared with a reduction in alumina content ($x=1$). It can be opined that second crystallization peak temperature (T_p^2) corresponds to a strongly surface nucleating phase i.e., strontium aluminum silicate.

An optimum nucleation temperature close to T_g is indicative of a nucleation mechanism occurring via prior amorphous phase separation [2]. Alumina will go into the glass network as a four coordinate ion and this requires an extra unit of positive charge to retain charge neutrality. Reduction in alumina content results in some of the alkali earth cations switching their role from charge balancing Al^{3+} ions to forming non-bridging oxygens. There is a consequent increase in the interruption of the formation of glass network and a fall in the crosslink density values, resulting in the reduction of glass transition temperature [15].

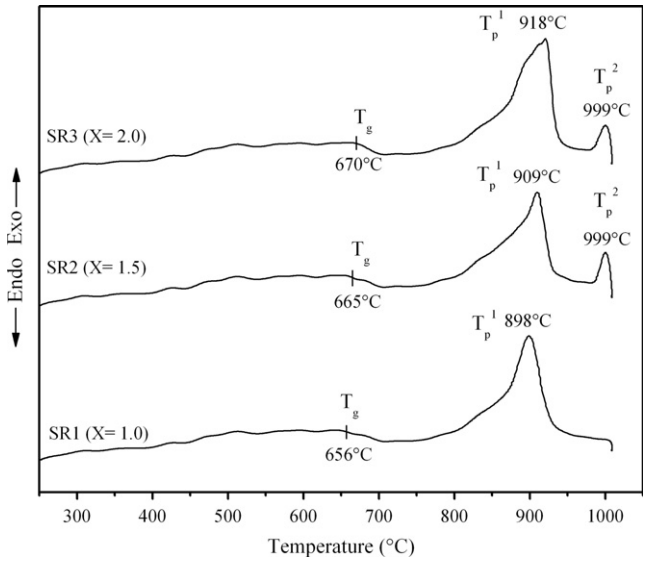

Fig. 1. Differential thermal analysis plots of glass samples at heating rate 10 °C/min for SR1, SR2 and SR3 batches.

3.2. X-ray diffraction

The JCPDS reference files were used to identify the various crystal phases formed. Amongst SR1, SR2 and SR3 batches, strontium fluorophlogopite and strontium aluminum silicate phases appear at all heat treatment temperatures and amount of these phases increases with increasing heat treatment as shown in Figs. 2–4. In all batches a hump of peak appears at 750 °C, which indicates the start of initial crystallization of above heat treated samples.

At 850 °C, only strontium fluorophlogopite phase appears but when temperature is increased to 950 °C, new peaks of strontium aluminum silicate, cordierite, mullite appear along with strontium fluorophlogopite in SR1 batch. At 1050 °C, the number of peaks of strontium aluminum silicate and cordierite increased along with strontium fluorophlogopite. At 1150 °C, there is no change in the intensity of the peaks and no new phase appeared but the sharpness of the peaks increased.

At 850 °C, strontium aluminum silicate phase appears along with strontium fluorophlogopite in SR2 batch. At 950 °C, there is no change in the intensity of the peaks and no new phases appeared. But when the temperature increases from 950 °C to 1050 °C, new peaks of cordierite and mullite appear along with strontium fluorophlogopite and strontium aluminum silicate. At 1150 °C, there is no change in the intensity of the peaks and no new phases appeared but the sharpness of the peaks increased.

At 850 °C, only strontium aluminum silicate phase appears along with strontium fluorophlogopite in SR3

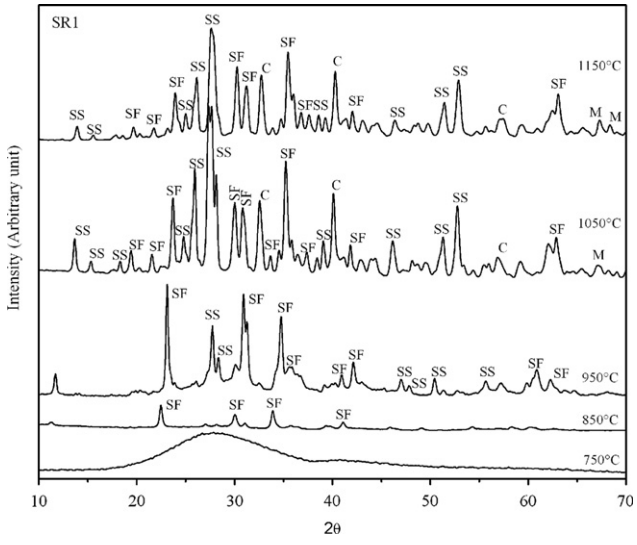

Fig. 2. XRD patterns for SR1 glass samples at different crystallization temperatures [SF—strontium fluorophlogopite (JCPDS ref. file-00-019-0117), SS—strontium aluminum silicate (JCPDS ref. file-00-010-0015), C—cordierite (JCPDS ref. file-00-012-0303) and M—mullite (JCPDS ref. file-00-001-0613)].

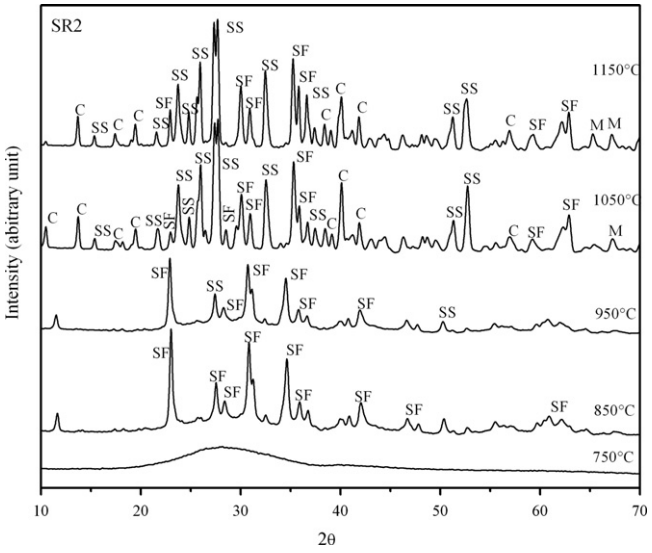

Fig. 3. XRD patterns for SR2 glass samples at different crystallization temperatures. [SF—strontium fluorophlogopite, SS—strontium aluminum silicate, C—cordierite and M—mullite].

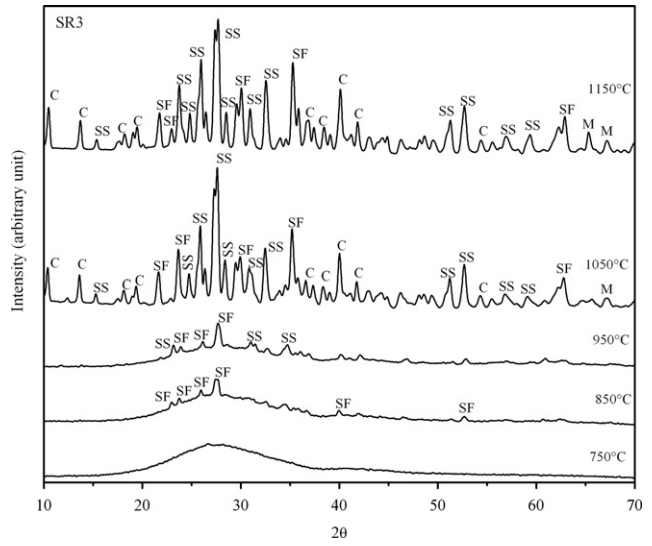

Fig. 4. XRD patterns for SR3 glass samples at different crystallization temperatures. [SF—strontium fluorophlogopite, SS—strontium aluminum silicate, C—cordierite and M—mullite].

batch. But when temperature is increased to 950 °C, new peaks of cordierite appear along with strontium aluminum silicate. At 1050 °C, new peaks of strontium fluorophlogopite, cordierite and mullite appear along with strontium aluminum silicate. At 1150 °C, there is no change in the intensity of the peaks and no new phases appeared but the sharpness of the peaks increased.

All the samples contain strontium fluorophlogopite as a major phase at 950 °C. At 1050 °C, both strontium fluorophlogopite and strontium aluminum silicate phases are present in SR1 and SR2 batches but strontium aluminum silicate is the major phase in SR3 batch. At 1150 °C, intensity of peaks for strontium fluorophlogopite and strontium aluminum silicate increased due to the crystal growth to large size.

The crystallizations of secondary phases rich in silica and alumina without fluorine, such as strontium aluminum silicate and cordierite, are formed at high temperatures (> 1050 °C) in SR1 and SR2 batches. But in SR3 batch, strontium aluminum silicate appeared as the major phase along with strontium fluorophlogopite, cordierite and mullite in all heat treatment temperatures. This may be an indication that higher alumina content favors the formation of the crystal phases rich in silica and alumina containing no fluorine, such as strontium aluminum silicate.

3.3. Microstructure analysis

In SR1–SR3 batches, samples heated at 750 °C for 5 h exhibit liquid–liquid phase separation. The liquid droplets are small and randomly distributed (Fig. 5a–c in order). Samples heated at 850 °C for 5 h exhibit very fine submicron microstructures and consist of some blocky crystals (Fig. 6a–c in order). But when the samples were heated at 950 °C for 5 h, they exhibited a large number of slightly bigger blocky crystals (Fig. 7a but not Fig. 7b and c) compared to those at 850 °C. These crystals are dense and appeared white in the back-scattered electron micrographs with more or less low aspect ratio in highly siliceous residual glass with acicular morphology.

Samples heated at 1050 °C for 5 h exhibited the appearance of lath like crystals with acicular morphology (Fig. 8a).

When alumina content is $x=1$, the mica crystals can coarsen and grow. In batch SR1 ($x=1$), a classic interconnected 'house of cards' microstructure with high aspect ratio could be produced at higher temperature i.e. 1150 °C (Fig. 9a). In batches SR1 and SR2 ($x=1.5$ and 2), a classic interconnected 'house of cards' microstructure with high aspect ratio could be produced at higher temperatures i.e. 1050 °C and 1150 °C (Figs. 8b, c and 9b, c). Higher alumina content ($x=1.5$ and 2) for batches SR2 and SR3 (Fig. 9b and c respectively) gave rise to a microstructure consisting of both small strontium fluorophlogopite crystals of 1–2 μm and much larger acicular mica crystals up to 14 μm in length.

4. Conclusion

Reduction in the alumina content reduces the glass transition temperature and first crystallization peak temperature, and promotes bulk crystallization. The first crystallization peak temperature corresponds to the crystallization of strontium fluorophlogopite in low alumina content batch. No precursor crystal phase was found prior to the formation of strontium fluorophlogopite. The second crystallization peak temperature corresponds to the crystallization of strontium aluminum silicate in

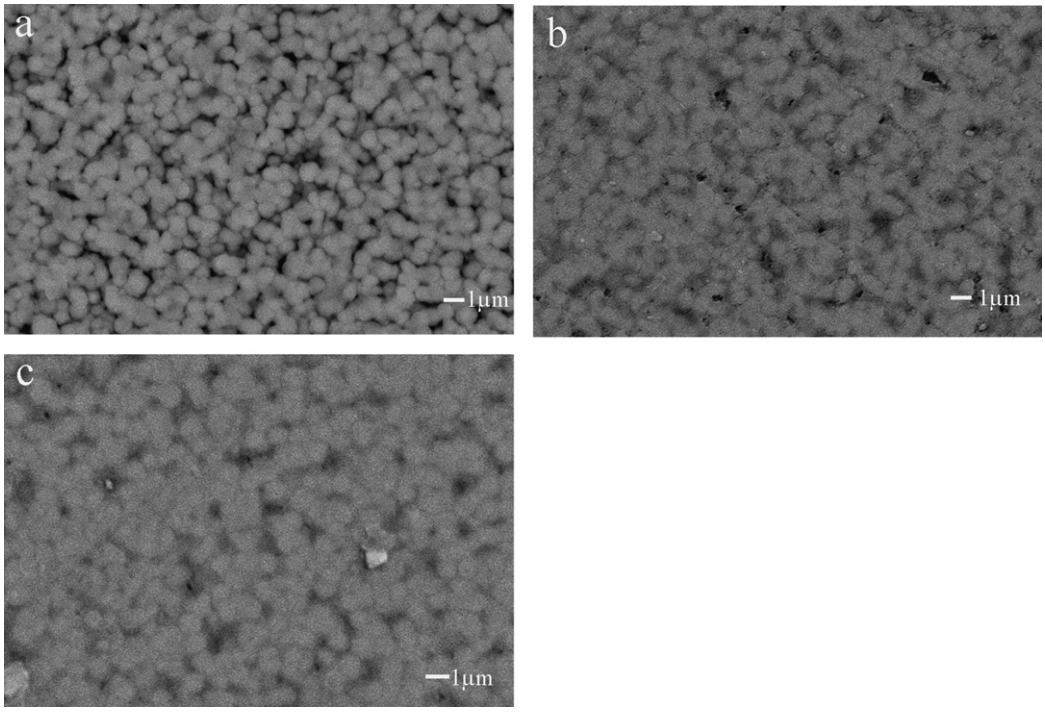

Fig. 5. (a). SEM photograph of polished and etched surface of SR1 samples crystallized at 750 °C for 5 h, (b). SEM photograph of polished and etched surface of SR2 samples crystallized at 750 °C for 5 h, and (c). SEM photograph of polished and etched surface of SR3 samples crystallized at 750 °C for 5 h.

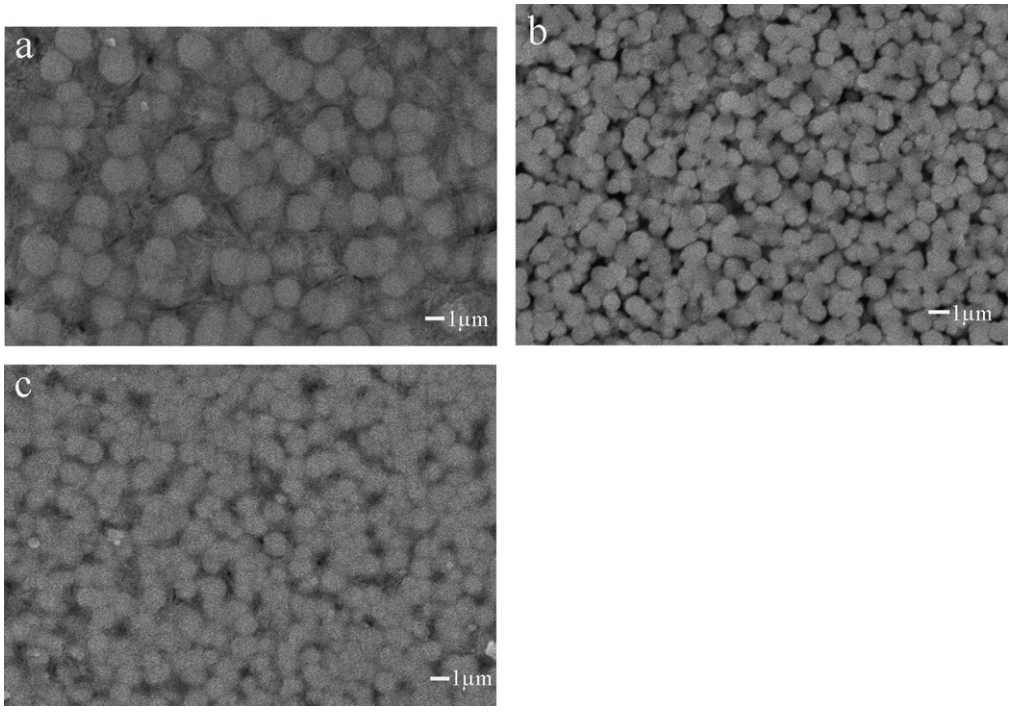

Fig. 6. (a). SEM photograph of polished and etched surface of SR1 samples crystallized at 850 °C for 5 h, (b). SEM photograph of polished and etched surface of SR2 samples crystallized at 850 °C for 5 h, and (c). SEM photograph of polished and etched surface of SR3 samples crystallized at 850 °C for 5 h.

high alumina content batch. High alumina contents favored the formation of strontium aluminum silicate, cordierite and mullite. Glasses with progressively high alumina content in batches SR2 and SR3, on heat treatment in the temperature range of 1050–1150 °C, gave microstructures consisting of elongated blocky crystals

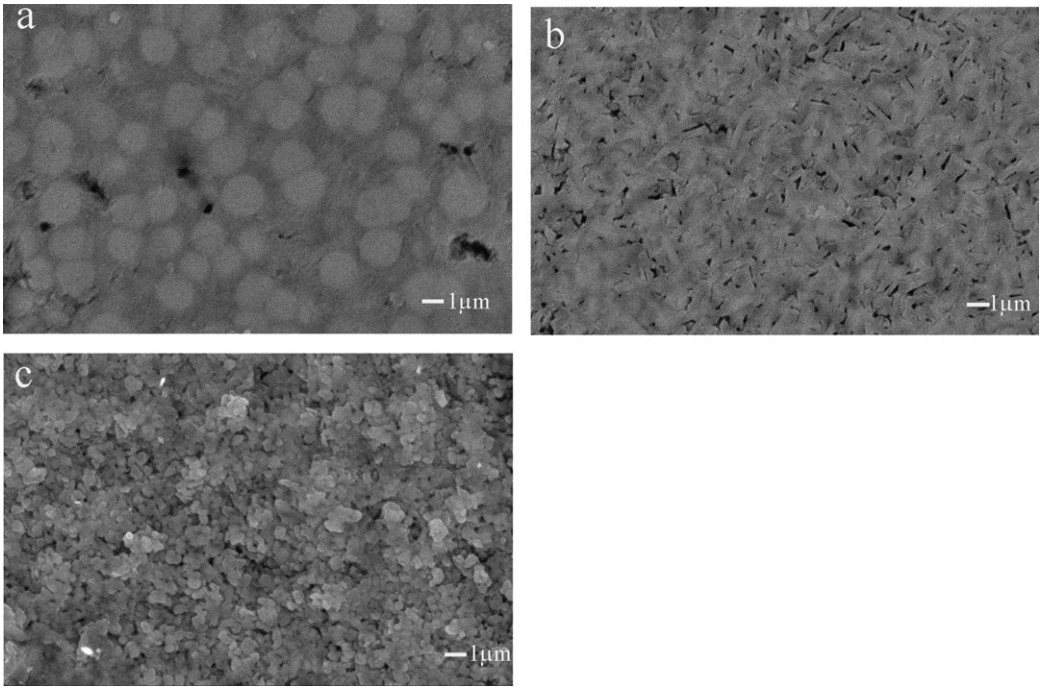

Fig. 7. (a). SEM photograph of polished and etched surface of SR1 samples crystallized at 950 °C for 5 h, (b). SEM photograph of polished and etched surface of SR2 samples crystallized at 950 °C for 5 h, and (c). SEM photograph of polished and etched surface of SR3 samples crystallized at 950 °C for 5 h.

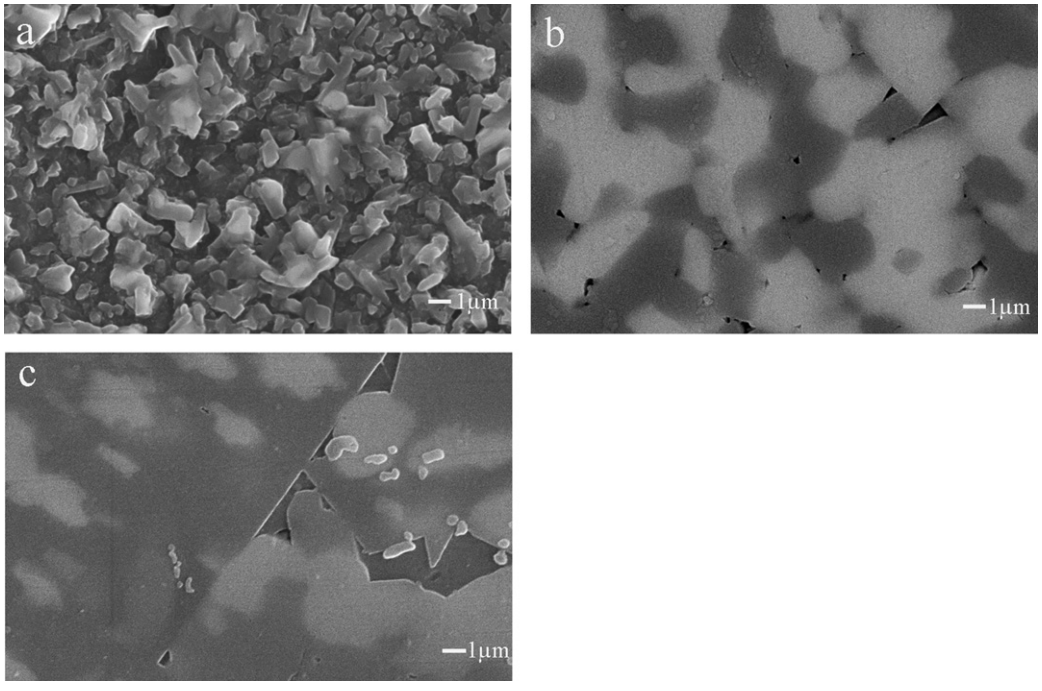

Fig. 8. (a). SEM photograph of polished and etched surface of SR1 samples crystallized at 1050 °C for 5 h, (b). SEM photograph of polished and etched surface of SR2 samples crystallized at 1050 °C for 5 h, and (c). SEM photograph of polished and etched surface of SR3 samples crystallized at 1050 °C for 5 h.

with a house of cards microstructure. The glass with low alumina contents (SR1) gave rise to blocky crystals of a high aspect ratio and therefore could not produce the classic house of cards microstructure at heat treatment temperature of 1050 °C but the classic house of cards microstructure was produced at heat treatment temperature of 1150 °C.

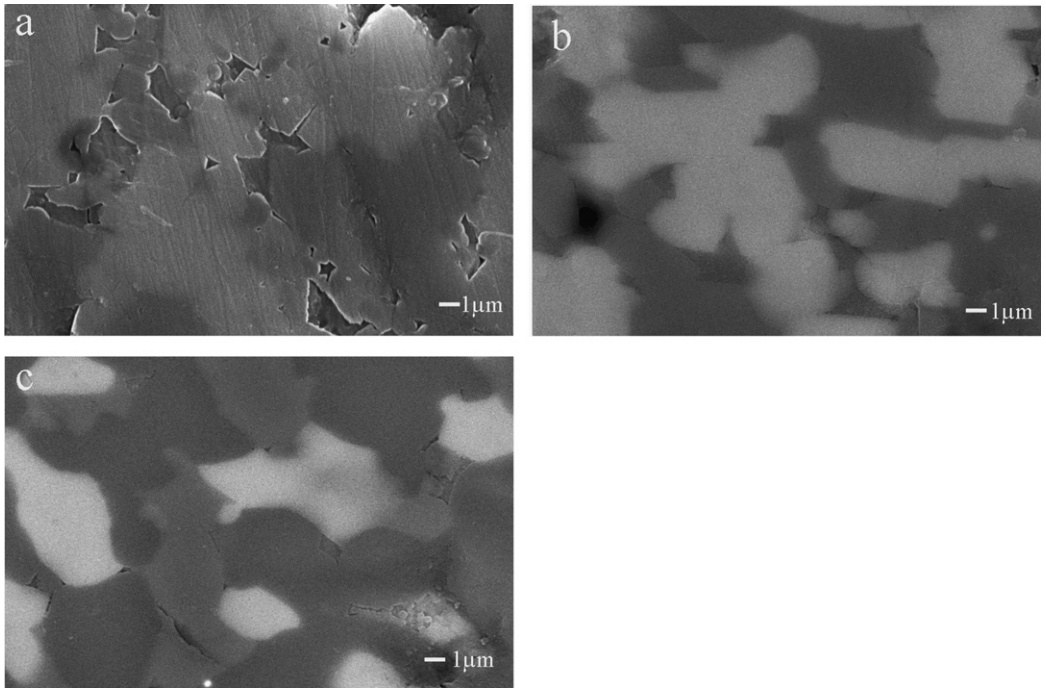

Fig. 9. (a). SEM photograph of polished and etched surface of SR1 samples crystallized at 1150 °C for 5 h, (b). SEM photograph of polished and etched surface of SR2 samples crystallized at 1150 °C for 5 h, and (c). SEM photograph of polished and etched surface of SR3 samples crystallized at 1150 °C for 5 h.

Acknowledgments

Financial support from the University Grants Commission (UGC), under Major Research Project, is gratefully acknowledged. SEM and XRD facilities were provided by Technical Education Quality Improvement Programme (TEQIP). AM thanks the UGC, New Delhi, India, for providing a Junior Research Fellowship (UGC-RGNF).

References

[1] D.S. Baik, K.S. No, J.S. Chun, Y.J. Yoon, H.Y. Cho, A comparative evaluation method of machinability for mica-based glass-ceramics, Journal of Materials Science 30 (1995) 1801–1806.
[2] P.W. Macmillan, in: Glass-Ceramics, second edition, Academic press, London, 1979.
[3] D.S. Baik, K.S. No, J.S. Chen, Y.J. Yoon, Mechanical properties of mica glass-ceramics, Journal of the American Ceramic Society 78 (1995) 1217–1222.
[4] C.K. Chyung, G.H. Beall, D.G. Grossman, Microstructure and mechanical properties of mica glass-ceramics, in: M. Kunugi, M. Tashiro, N. Saga (Eds.), Tenth International Congress on Glass, Ceramic Society of Japan, Kyoto, Japan, 1974, pp. 1167–1194 Part 11.
[5] C.K. Chyung, G.H. Beall, D.G. Grossman, Fluorphlogopite mica glass-ceramics, in: Proceedings of the International Glass Congress, No. 14, Kyoto, Japan, Ceramic Society of Japan, Tokyo, Japan, 1974, pp. 33–40.
[6] T. Uno, T. Kasuga, K. Nakajima, High-strength mica containing glass-ceramics, Journal of the American Ceramic Society 74 (1991) 3139–3143.
[7] W. Holand, W. Vogel, W.J. Mortier, A new type of phlogopite crystals in machinable glass-ceramics, Glass Technology 24 (1983) 318–322.
[8] D.G. Grossman, Machinable glass-ceramics based on tetrasilisic mica, Journal of the American Ceramic Society 55 (1972) 446–449.
[9] K. Greene, M.J. Pomeroy, S. Hampshire, R. Hill, Effect of composition on the properties of glasses in the K_2O–BaO–MgO–SiO_2–B_2O_3–MgF_2 system, Journal of Non-Crystalline Solids 325 (2003) 193–205.
[10] P.K. Maiti, A. Mallik, A. Basumajumdar, P. Guha, Influence of barium oxide on the crystallization, microstructure and mechanical properties of potassium fluorophlogopite glass-ceramics, Ceramics International 38 (2012) 251–258.
[11] P.K. Maiti, A. Mallik, A. Basumajumdar, P. Kundu, Influence of fluorine content on the crystallization and microstructure of barium fluorophlogopite glass-ceramics, Ceramics International 36 (2010) 115–120.
[12] A. Mallik, P.K. Maiti, P. Kundu, A. Basumajumdar, Influence of B_2O_3 on crystallization behavior and microstructure of mica glass-ceramics in the system $BaO \cdot 4MgO \cdot Al_2O_3 \cdot 6SiO_2 \cdot 2MgF_2$, Journal of the American Ceramic Society 95 (2012) 3505–3508.
[13] G.H. Beall, in: L.L. Hench, S.W. Frieman (Eds.), Advances in Nucleation and Crystallization in Glasses, Journal of the American Ceramic Society, Westerville, (1971) p. 251.
[14] S.N. Hoda, G.H. Beall, in: J.H. Simmons, D.R. Uhlmann (Eds.), Alkaline earth mica glass ceramics, Advances in Ceramics: Nucleation and Crystallization in Glasses, Journal of the American Ceramic Society 2 (1982) pp. 287–300.
[15] J. Henry, R.G. Hill, Influence of alumina content on the nucleation crystallization and microstructure of barium fluorophlogopite glass-ceramics based on $8SiO_2 \cdot YAl_2O_3 \cdot 4MgO \cdot MgF_2 \cdot BaO$. Part I. Nucleation and crystallization behavior, Journal of Materials Science 39 (2004) 2499–2507.
[16] J. Henry, R.G. Hill, Influence of alumina content on the nucleation crystallization and microstructure of barium fluorophlogopite glass-ceramics based on $8SiO_2 \cdot YAl_2O_3 \cdot 4MgO \cdot 2MgF_2 \cdot BaO$. Part II. Microstructure, microhardness and machinability, Journal of Materials Science 39 (2004) 2509–2515.